SMAR 2017 – Fourth Conference on Smart Monitoring,
Assessment and Rehabilitation of Civil Structures

Fatigue life prediction of RC beams strengthened with FRP through MLE method

Leila Cristina Meneghetti[1], Mônica Regina Garcez[2], Ritermayer Monteiro Teixeira[1] and Luiz Carlos Pinto da Silva Filho[2]

[1] University of São Paulo, São Paulo, Brazil
[2] Federal University of Rio Grande do Sul, Porto Alegre, Brazil

ABSTRACT: The use of externally bonded FRP increases the fatigue life of RC beams due to the reduction of the steel stress level if compared to unstrengthened beams. For steel stresses up to 80% of yield stress, fatigue failure is normally marked by the gradual deterioration of the steel rebars, which leads a stress transfer to the FRP, until failure. Higher steel stresses are associated with FRP debonding, while steel stresses below the fatigue limit will never lead to fatigue failure. In this paper, the Maximum Likelihood Estimation Method (MLE) was used to determine S-N curves aiming to predict fatigue life of RC beams strengthened with FRP. Experimental data with runouts of fatigue tests found in literature were used to adjust the fatigue model aiming to characterize the large scatter between the results of fatigue tests from the different sources. The proposed fatigue model represents accurately the declivity of the fatigue curve for FRP strengthened beams.

1 INTRODUCTION

Cyclic loading are one of the main causes of RC deterioration in bridges because repeated loading and unloading cycles may lead to fatigue (Demers, 1998; Ye et al., 2014; Song and Yu, 2015). Fatigue has an important effect on RC structures since it may significantly reduce the expected lifetime, resulting in catastrophic failure even with applied loads below the structural capacity of the elements. Although FRP strengthening design methods are now established and many guidelines exist, fatigue design procedure is still an ongoing research topic. Considering that a typical RC highway bridge deck with a design life of 40 years may experience a minimum of 58 x 108 loading cycles of varying intensities (Ferrier et al., 2012), the behavior of such structures under fatigue is of fundamental importance.

A considerable effort has been expended to assess the fatigue behavior of RC members strengthened with FRP, including: dynamic deboning failure mechanism (Mulian and Rabinovitch, 2016), fatigue behavior under aggressive environments (Qin et al., 2016; Song Yu, 2015), different FRP configuration and load ranges (Charalambidi, 2016; Peng et al., 2016; Gheorghiu et al., 2007; Gussenhoven and Breña, 2005; Quattlebaum et al., 2005; Barnes and Mays, 1999), as well as prestressed FRP (Peng et al., 2016; Oudah and El-Hacha, 2013). Although widely used, fatigue tests are time-consuming and expensive. Curve fitting of fatigue data is also time-consuming. On the other hand, engineering designers need to make safe use of these complex fatigue life data, especially for unconventional materials like composites. Therefore, fatigue analytical models can link theoretical ideas with the observed data to provide a good prediction of future observations (Ye et al., 2014) or even can be useful for deciding aspects to be explored in real scale fatigue tests.

Linear regression analysis (LRA) is widely used to generate fatigue models for strengthened beams. However, oftentimes, a predicted number of cycles is applied to assess the fatigue behavior of a structural element (Aidoo et al., 2004; Gheorghiu et al., 2007; Wang et al., 2007) or even tests are interrupted before the failure (Gussenhoven and Breña, 2005; Charalambidi et al., 2016) which generate runouts data. Such data are not used in classical regression analysis since the number of load cycles at failure is unknown and the number of load cycles at which the test was interrupted is completely arbitrary (Taras & Greiner, 2009). Furthermore, the constant amplitude fatigue limit (CAFL) position is arbitrarily chosen and prediction bounds of linear regression curves are based on fatigue data scatter in the finite-life region resulting in less accuracy in the high cycle fatigue region (D'Angelo et al., 2014). Nevertheless, in the statistical viewpoint, runouts represent a special type of data, so-called censored data. This type of data is not as complete as test data resulting from a fatigue test that led to a failure, but also show that the tested member could achieve more than the number of load cycles at the test interruption.

A suitable statistical method to include this valuable information is the Maximum Likelihood Estimation (MLE) that will be used in this paper to determine S-N curves and confidence intervals for beams strengthened with FRP. Experimental data with runouts of fatigue tests found in literature and generated through an experimental program are used to adjust the fatigue model aiming to characterize the large scatter between the results of fatigue tests from the different sources. Fatigue models based on linear regression analysis are compared to the ones generated through the Maximum Likelihood Method (MLE).

2 BASIS FOR S-N DESIGN CURVES

Considering that a straight line in log-log scale represents the stress range versus the number of cycles within a specific interval, S-N relationships may be obtained using a classical statistical analysis based on random data set. The average S-N curve is obtained through a linear model according to Eq.1, where $y = \log(\Delta\sigma)$ denotes the independent variable, and $\Delta\sigma$ is the stress range; A and B are the intercept and the slope of the S-N curve in the log-log scale and $\bar{x}$ denotes the average values of $\log(N)$, being N is the number of cycles to failure.

$$\bar{x} = B \cdot y + A \qquad (1)$$

The relation expressed by Eq. 1 is associated to a 50th percentile of failure, considering that $\log(N)$ is a normally distributed random variable. In order to obtain S-N curves for others percentiles, a linear prediction bound can be determined around the mean regression line computing the sample standard S deviation of $\log(N)$ and multiplying it by a factor α, as expressed by Eq. 2.

$$\bar{x} = B \cdot y + \left(A \pm \alpha \cdot S\right) \qquad (2)$$

In this paper, α = -1.645 and α = -0.675 were used, respectively, for fifth e 25th percentiles. The 5% probability of failure corresponds to the S-N design curves (CEB-FIP, 2010).

According to ASTM E739-10 (2015), linear regressions are carried out following some assumptions: (a) the database collected constitutes a random sample from a population of all possible test results; (b) the individual results, in terms of fatigue life, are random samples from a lognormal population. A random sample is required for a meaningful evaluation of population parameters, confidence limits and tolerance intervals. The second assumption implies that the predict variable (fatigue life), transformed logarithmically, will become normally distributed, a requirement for using the variance of the error to determine the significance of the regression parameters.

The fatigue model generated through Eq. 1 and 2 fits the experimental dataset collected using the least square method. In this case, only failure points are considered. The normally distributed parameters of the fatigue model, B and A, are estimated using Eq. 3 and 4, where μ_y and μ_x denote the average of experimental values y_i and x_i, respectively, and n is the total number of test specimens.

$$B = \sum_{i=1}^{n} \frac{\left(y_i - \mu_y\right)\cdot\left(x_i - \mu_x\right)}{\left(y_i - \mu_y\right)^2} = \frac{S_{yx}}{S_{yy}} \tag{3}$$

$$A = \mu_x - B \cdot \mu_y \tag{4}$$

The standard deviation S of $\log(N_i)$ can be determined by means of variance of the normal distribution as shown in Eq. 5.

$$S^2 = \frac{\sum_{i=1}^{n}[x_i - \overline{x}(y_i)]^2}{n-1} \tag{5}$$

In the fatigue field, Pascual and Meeker (1999) proposed a five-parameter random fatigue limit model using MLE. When applied to fatigue, the method determines the S-N curve that describes the most likely location of each fatigue test result, including runouts.

For the random fatigue-limit model, Eq. 6 gives the likelihood function.

$$\Gamma(\theta) = \prod_{i=1}^{n} \left[f(z_i;\theta)\right]^{\delta_i} \left[F(z_i;\theta)\right]^{1-\delta_i} \tag{6}$$

Where: $\delta_i \begin{cases} 1 \text{ for failure} \\ 0 \text{ for run-out} \end{cases}$ and $z_i = \left[x_i - \overline{x}(y_i)\right]/S$. Functions $f(z_i;\theta)$ and $F(z_i;\theta)$ denote, respectively, the probability density and the cumulative probability distribution of z_i. $\theta = [A \quad B \quad S]$ is the vector of the optimization parameters.

Generally, it is easier to work with the log-likelihood function, because in this form the maximization is made by a sum instead of a product. Assuming that data may be adjusted through a normal log-log scale distribution, the log-likelihood function $L_i(\theta)$ for a single test result is given by Eq. 7.

$$L_i(\theta) = \delta_i \left\{\log\left[f(z_i;\theta)\right] - \log\left[S \cdot N_i\right]\right\} + (1-\delta_i)\log\left[1 - F\left(z_i;\theta\right)\right] \tag{7}$$

Thus, the log-likelihood function of all dataset $\Lambda(\theta) = \log\left[\Gamma(\theta)\right]$ is given by the contribution of each single test, according to Eq. 8.

$$\Lambda(\theta) = \sum_{i=1}^{n} L_i(\theta) \tag{8}$$

θ Must be determined to maximize function $\Lambda(\theta)$. In this paper a script was developed using MATLAB Optimization Toolbox™ (The Mathworks, 2010), aiming to solve constrained nonlinear minimization problems, including active-set and interior-point optimization algorithms. Such algorithms may be used to maximize $\Lambda(\theta)$ (or to minimize $-\Lambda(\theta)$) when initial constraints are given to θ, in order to limit the search space within a physically possible region.

3 FATIGUE DATABASE

Experimental data of fatigue tests with runouts, reported by Papakonstantinou et al. (2001), Aidoo et al. (2004), Heffernan and Erki (2004), Gussenhoven and Breña (2005), Toutanji et al. (2006), Gheorghiu et al. (2007), Wang et al. (2007), Meneghetti (2008) and Charalambidi et al. (2016), were used to generate the proposed fatigue models. Tables 1 shows the fatigue data used to generate the proposed fatigue models.

Table 1. Summary of fatigue data (part 1).

	Specimen	**FRP system**	**Steel Stress Range MPa**	**Number of cycles**	**Failure 1-yes 0-no**
Papakonstantinou et al. (2001)	S-2	GFRP sheets	266	880,000	1
	S-5		268	800,000	1
	S-6		359	126,000	1
	S-7		299	570,000	1
	S-8		454	30,500	1
	S-9		325	235,000	1
	S-10		246	685,000	1
Heffernan and Erki (2004)	LCFa	CFRP prepreg	160	4,890,000	1
	LCFb		160	6,440,000	1
	MCFa		201	900,000	1
	MCFb		201	890,000	1
	HCFa		241	340,000	1
	HCFb		241	390,000	1
	CF-2	CFRP sheets	215	312,000	1
	CF-4		202	627,000	1
	CF-6		191	1,049,000	1
Aidoo et al. (2004)	RS1	CFRP sheets	338	308,879	1
	RS2		279	1,280,000	1
	RF1	CFRP strips	306	193,160	1
	RF2		279	960,000	1
Wang et al.(2007)	C2	GFRP CFRP strips sheets	200	1,000,000	0
Gheorghiu et al. (2007)	H2000A	CFRP strips	254	2,000,000	0
	H2000B		267	2,000,000	0

Table 1. Summary of fatigue data (part 2).

	Specimen	FRP system	Steel Stress Range MPa	Number of cycles	Failure 1-yes 0-no
Toutanji et al. (2006)	3FI-9	CFRP sheets	283	259,432	1
	3FI-10		283	314,728	1
	3FI-11		283	197,954	1
	3FI-12		367	74,383	1
	3FI-13		367	74,579	1
	3FI-14		398	2,122	1
	3FI-15		398	2,375	1
	3FI-16		398	4,480	1
	3FI-17		398	5,047	1
Charalambidi et al. (2016)	REX20-L	CFRP sheets	220	2,000,000	0
	TEX20-L		220	1,300,000	0
	REX20-H		352	990,147	1
	REX40-H		365	1,450,105	1
	RNSM20-H	CFRP strips	352	807,437	1
	RNSM40-H		373	696,500	1
	TNSM20-H		340	774,411	1
Gussenhoven et al. (2005)	A-1-4-80	CFRP sheets	295	13,1619	1
	A-1-4-70		272	28,7594	1
	A-1-4-60		224	778,734	1
	B-1-2-80		300	290,307	1
	B-1-2-70		268	336,873	1
	B-1-2-60		236	4,000,000	0
	B-2-2-70		270	150,000	1
	B-2-2-60		199	2,000,000	0
	C-1-2-80S		326	326,775	1
	C-1-2-70S		226	4,401,793	1
	C-1-2-60S		189	4,000,000	0
Meneghetti (2007)	CA	CFRP sheets	310	210,217	1
	CB		246	378,499	1
	AA	AFRP sheets	312	234,368	1
	AB		247	665,609	1
	VA	GFRP sheets	258	832,517	1
	VB		204	3,662,726	1
	CB1	CFRP sheets	338	258,515	1
	CB2		338	208,928	1
	CB3		338	217,026	1
	CA1		203	4,999,750	0
	CD1		203	5,000,000	0
	CC1		68	4,871,000	0
	AB1	AFRP sheets	387	212,201	1
	AA1		232	5,000,000	0
	AC2		232	5,081,300	0
	AD1		77	5,000,000	0
	VB1	GFRP sheets	347	137,250	1
	VA2		208	2,384,018	1
	VA3		208	5,000,000	0
	VC1		208	885,000	1
	VC2		208	5,000,000	0

4 S-N CURVES

The LRA model was generated using data from 51 samples and 15 runouts were included to generate the MLE model. Fig. 2 shows S-N curves considering LRA based average, 25%, and 5% percentiles, while Fig. 2 shows S-N curves with MLE based average, 25%, and 5% percentiles.

LRA and MLE average S-N curves (Fig. 2) fit for most of data. The slopes for LRA are higher than the observed using MLE. Due to this fact, the LRA model becomes more conservative if compared to the MLE. The average LRA S-N curve estimates 176,54MPa at 2 million cycles while the MLE approach estimates 215.28MPa, as showed in Table 6. Values obtained through 25% and 5% percentiles S-N curves at 2 million cycles decreases to 149.0MPa and 116.77MPa, respectively, (LRA) and to 184.56MPa and 147.65MPa, respectively, (MLE).

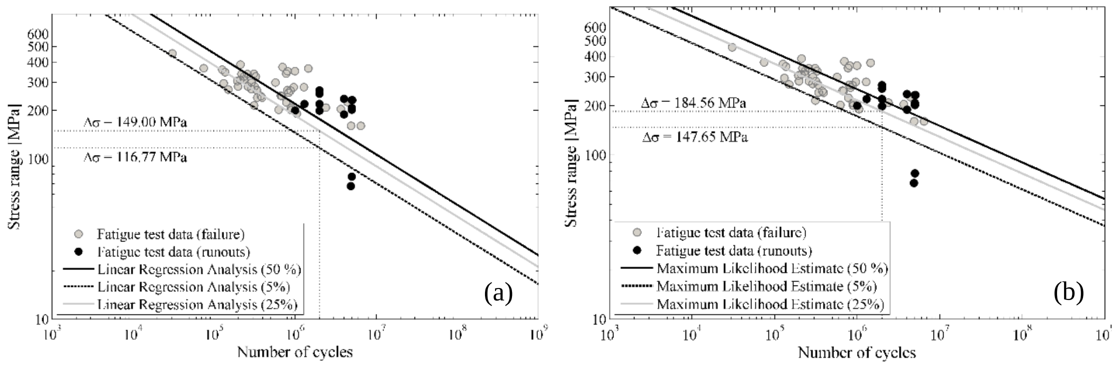

Figure 2. (a) Linear regression analysis for all failure points; (b) Maximum likelihood estimation for all database.

The 5% percentile S-N curve obtained through MLE is relatively closed to the fatigue test results between 105 and 106 ( ), but diverges from the results in which minimum stress level is outside this range. The most appropriate S-N curve to fit the whole cloud of data points and stress range with percentile 5% is not given by a straight line, but by a curve (m <- 4.48 over 2 million cycles and m> -4.48 in the high stress range).

The best S-N curve fitting, obtained with MLE, considering the whole cloud of data points, seems to be associated to the inclusion of runouts with low stress range and number of cycles higher than 5,000,000. The existence of two points associated to a stress range lower than 100MPa in which tests were interrupted when 5,000,000 cycles were reached, indicates that the specimen could support a number of cycles much higher, with the possibility to achieve infinite fatigue lifetime.

The fatigue endurance limit for unstrengthened beams given by ACI 215 (1997) may be estimated using the equation , where □smin is the minimum steel stress level, pointing out that stress variations lower than 138 MPa could be ignored. Results of Table 6 seem to indicate that FRP strengthening could have a positive effect on the endurance limit of the original steel rebars, due to stress redistribution. In such case, fatigue damage is unlikely when stress variation is lower than 200 MPa, if the maximum load is not excessive (higher than 85% of ultimate load capacity). However, given the large scatter of fatigue data and the reduced size of the database available, further tests and confirmation of this tendency are necessary before any consideration of a higher endurance limit for strengthened beams is made.

5 CONCLUSIONS

Based on experimental results from an extensively experimental program and additional data gathered from the literature, it was possible to adjust models based on LRA and MLE method. MLE and LRA S-N curves showed different declivity, indicating that LRA leads to a more conservative estimative, probably because runouts are not considered in LRA.

The 5% percentile S-N curve obtained through MLE seems to be more appropriate to estimate fatigue lifetime for stress ranges between 172MPa e 288MPa. For lifetimes over two million cycles and stress ranges lower than 172MPa, S-N curves should be fitted to a lower declivity, resulting in a flatter shape.

In the large majority of cases, fatigue failure is primarily associated with an initial steel rebar fracture and the magnitude of the steel stress range is the main factor determining fatigue life, as it is well known for unstrengthened RC beams. Nonetheless, data seems to suggest that the use of FRP strengthening can shift slightly upward the steel rebars endurance limit. More fatigue tests data with strengthened RC beams submitted to different steel stress ranges are needed to ratify these findings

REFERENCES

ACI 215 (1997). Considerations for Design of Concrete Structures Subjected to Fatigue Loading. American Concrete Institute. Farmington Hills.

Aidoo J, Harries KA and Petrou MF (2004) Fatigue behavior of carbon fiber reinforced polymer strengthened reinforced concrete bridge girders. Journal of Composites for Construction 8(6): 501-509

ASTM D3039/D3039M (2006). Standard Test Method for Tensile Properties of Polymer Matrix Composites Materials. ASTM International, West Conshohocken, PA.

ASTM E739-10 (2015). Standard Practice for Statistical Analysis of Linear or Linearized Stress-Life (S-N) and Strain-Life (ε-N) Fatigue Data. ASTM International, West Conshohocken, PA.

Barnes R A, Mays G C (1999) Fatigue performance of concrete beams strengthened with CFRP plates. Journal of Composites for Construction 3(2): 63-72.

CEB-FIP (2010). Model Code 2010: First Complete Draft Volume 2. International Federation for Structural Concrete (fib). Lausanne, Switzerland.

Charalambidi BG, Rousakis TC and Karabinis AI (2016) Fatigue behavior of large-scale reinforced concrete beams strengthened in flexure with fiber-reinforced polymer laminates. Journal of Composites for Construction 20(5): 69-78.

D'Angelo L, Rocha M, Nussbaumer A (2014) S-N-P fatigue curves using maximum likelihood method for fatigue resistance curves with application to straight and welded rebars. Proceeding of Seventh European Conference on Steel and Composite Structures. ECCS European Convention for Constructional Steelwork, Brussel, Belgium.

Demers C E (1998) Fatigue strength degradation of E-glass FRP composites and carbon FRP composites. Construction and Building Materials 12: 311-318.

Ferrier E, Bigaud D, Clément J C and Hamelin P (2012) Fatigue-loading effect on RC beams strengthened with externally bonded FRP. Construction and Building Materials 25 (2): 539-546.

Gheorghiu C, Labossière P and Proulx, J (2007) Response of CFRP-strengthened beams under fatigue with different load amplitudes. Construction and Building Materials 21: 756-763.

Gussenhoven R and Breña SF (2005) Fatigue Behavior of Reinforced Concrete Beams Strengthened with Different FRP Laminate Configurations. American Concrete Institute, Farmington Hills, MI, USA, SP 230-36 pp. 613–630.

Heffernan PJ and Erki MA (2004) Fatigue behavior of reinforced concrete beams strengthened with carbon fiber reinforced plastic laminates. Journal of Composites for Construction 8(2): 132-140.

Meneghetti L C (2007) Análise do comportamento à fadiga de vigas de concreto armado reforçadas com PRF de vidro, carbono e aramida. Thesis. Department of Civil Engineering, Federal University of Rio Grande do Sul, Porto Alegre, Brazil.

Muliana G and Rabinovitch O (2016) Experimental and analytical study of the dynamic debonding in FRP plated beams. International Journal of Solids and Structures 92-93: 121–134.

Oudah F and El-Hacha R (2013) Fatigue behavior of RC beams strengthened using FRP in flexure: state-of-the-art review. Composites Part B: Engineering 47: 82–95.

Papakonstantinou C G, Petrou MF and Harries, KA (2001) Fatigue behavior of RC beams strengthened with GFRP sheets. Journal of Composites for Construction 5(4): 246-253.

Pascual F G and Meeker W Q (1999) Analysis of Fatigue Data with Runouts Based on a Model with Nonconstant Standard Deviation and a Fatigue Limit Parameter. Statistics Preprints. See http://lib.dr.iastate.edu/stat_las_preprints/3 (accessed 25/07/2016).

Peng H, Zhang J, Shang S, Liu Y and Cai F C S (2016) Experimental study of flexural fatigue performance of reinforced concrete beams strengthened with prestressed CFRP plates. Engineering Structures 127: 62–72.

Qin G, Huang P, Zhou H, Guo X and Zheng X (2016) Fatigue and durability behavior of RC beams strengthened with CFRP under hot-wet environment. Construction and Building Materials 111: 735–742.

Quattlebaum J B, Harries K A and Petrou M F (2005) Comparison of three flexural retrofit systems under monotonic and fatigue loads. Journal of Bridge Engineering 10(6): 731-740.

Silva Filho L C P (1999) Ttowards advanced bridge management systems: investigation of the possibility of developing an improved appraisal model based on a novel system architecture. Thesis. Department of Civil Engineering, University of Leeds, Leeds, UK.

Song L and Yu Z (2015) Fatigue performance of corroded reinforced concrete beams strengthened with CFRP sheets. Construction and Building Materials 90: 99–109.

Taras A and Greiner R (2009) Development and application of a fatigue class catalogue for Riveted Bridge components. Institute for Steel Structures and Sheel Structures. Graz University of Technology, Graz, Austria, ECCS TC6-2009, pp. 1–47.

The Mathworks (2010). Optimization Toolbox™ User's Guide (Release 2010b). The Mathworks Inc, Natick, Massachusetts, United States.

Toutanji H, Zhao L, Deng Y, Zhang Y. and Balaguru P (2006) Cyclic behavior of RC beams strengthened with carbon fiber sheets bonded by inorganic matrix. Journal of Materials in Civil Engineering 18(1): 28-35.

Wang YC, Lee M. and Chen BC (2007) Experimental study of FRP-strengthened RC bridge girders subjected to fatigue loading. Composites Structures 81(4): 491-498.

Ye X W, Su Y H and Han J P (2014) A state-of-the-art review on fatigue life assessment of steel bridges. Mathematical Problems in Engineering: 1-13.